

Crystallinity variations in kaolinite induced by grinding and pressure treatments

A. La IGLESIA

Instituto Geologia Economica CSIC, Facultad de Ciencias Geologicas, UCM E-28040-Madrid, Spain

A. J. AZNAR

E.P.S., Univ. Carlos III de Madrid, Butarque, 15, E-28911-Leganés, Spain

Kaolinite samples treated with uniaxial pressures higher than 0.1 GPa or grinding times greater than 0.3 h show changes in their crystallinity. These changes are easily detected by the X-ray diffraction (XRD) technique and can be quantified from Hinckley (HI), Lietard (R_2) and also reference intensity ratio (RIR) index studies. The sensitivity of these indices to the crystallinity changes is; $HI > RIR > R_2$. In the range of pressures and grinding times considered, these values can be diminished by 50%. The variations in these indices with either the pressure or grinding time follow logarithmic laws whose correlation coefficients are closed to unity. Infrared (IR) spectroscopy and thermal analysis studies show low sensitivity to the changes introduced by grinding or pressure. Nevertheless, thermal gravimetric curves confirm the decrease in the dehydroxylation starting point of about 100 °C for the pressed and ground samples. Transmission electron microscopy (TEM) reveals important changes in kaolinite particle morphologies after pressure and grinding treatments. The samples compressed at 0.1, 0.32, 0.85, 1.0 and 2.0 GPa show a large number of defects (fractures, bending, deformations and rolling of layers, glide and rotation of the shell). The ground samples show grain boundaries, dislocations, twins and rounded voids. These defects are responsible for the decrease in crystallinity of the kaolinite samples shown in the XRD and IR studies.

1. Introduction

It is well known that grinding kaolinite: (1) changes both the size and shape of the particles; (2) decreases crystallinity and induces structural changes such as polymorphic transformations or even total structure disorder; and (3) affects physico-chemical properties (specific surface, cation exchange capacity, water absorption, acidic media solubility, [1–8]). It has also been clearly established that high static pressures decrease the crystallinity of fragile materials in a similar way to that induced by grinding. There are only a few papers focusing on the effects induced by high pressures on the crystallinity and the physico-chemical properties of kaolinite. Thus, reference (9) and recently reference (10) have applied X-ray diffraction (XRD) and transmission electron microscopy (TEM) techniques to study the effect of high static pressure (in the range from 0.1–2.0 GPa) in kaolinite. These investigations showed that the application of high pressures produces strong crystalline disorder in kaolinite. We report here results concerning the effects of both pressure and grinding on the crystallinity, thermal properties and morphology of different samples of kaolinite.

2. Experimental procedure

Four samples have been studied: (1) Caobar kaolinite from Poveda de la Sierra (Guadalajara, Spain) which

was studied in reference [11] and described in reference [12]; (2) Georgia kaolinite (Georgia, USA) studied in reference [13]; (3) Majadas and (4) Valdecabras kaolinite (Cuenca, Spain) both studied and described in reference [11].

Sample grinding was accomplished in a Glen Greston vibrator built from tungsten carbide. A weight of 0.5 g of kaolin for time periods from 1–12 h were employed in the experiments.

For the pressure experiments a home-made cell was employed. This cell consisted of a cylinder of 60 mm in diameter housing two 13 mm (diameter) face to face pistons, built in F-522 steel to allow a maximum uniaxial pressure of 2.0 GPa in a volume of 1 ml.

Chemical analysis of the samples was carried out by conventional methods. The concentrations of aluminium, iron, titanium, calcium and magnesium were determined by atomic absorption spectroscopy. The sodium and potassium contents were measured by emission spectroscopy whilst the silica content was deduced by gravimetry.

Powder X-ray diffraction patterns of the samples were recorded on a Philips PW 1710 diffractometer using CuK_α radiation. The crystal perfection degree amongst the kaolinite samples was estimated from XRD data by determining the following parameters: the Hinckley index (HI) [14], the Lietard index (R_2)

[15], and the reference intensity ratio (RIR). The Hinckley index is based on the measurements of 020, $1\bar{1}0$ and $11\bar{1}$ reflections and the Lietard index on the measurement of 131 and $1\bar{3}1$ reflections. The reference intensity ratio (RIR) was estimated according to the methods of references [16, 17]. The three strongest peaks in both analyses (001, 002 and $1\bar{1}0$ reflections) and α -alumina used as a reference material (012, 104 and 113 reflections) were used in a 1:1 weight mixture. A technique for using any number of peaks to determine the RIR value is the normalized peak height ratio in the pure phase patterns of each material. These values are then used to convert each analysed intensity I_i^{rel} of the mixture to an equivalent intensity I_i^{100} of the strongest peak, [18]. To analyse the component i this process is represented by:

$$I_i^{100} = \frac{1}{n} \sum_{i=1}^n \frac{100 I_i^{\text{rel}}}{r_i}$$

where r_i is the normalized peak intensities from the pure phase patterns and n is the number of peaks used. According to references [16, 17] this method produces more reproducible results than an RIR computation from the mixture pattern using only single peaks.

Differential thermal analysis (DTA) and thermogravimetric analyses (TGA) were carried out using a Stanton 780 instrument. About 10 mg of sample and a 10°C per min heating rate were employed in the experiments. Calcined kaolinite was used as reference material.

Infrared spectra in the $4000\text{--}400\text{ cm}^{-1}$ range were recorded on a Mattson FTIR 3000 spectrophotometer. The pressed KBr pellet technique was used. A milligram of air dried kaolinite (105°C for 18 h) was added to 200 mg of KBr. Changes in the $960\text{--}750\text{ cm}^{-1}$ region, which includes bending vibrations involving hydroxyl groups and octahedral aluminium [19], were used to evaluate the variation in crystallinity.

Pressed samples of the Caobar and Georgia kaolinites were examined in a Jeol 2000 FX electron microscope. Ground samples were studied in a Philips 300 electron microscope. In both cases the dispersion of the kaolinite crystals was prepared by sonication.

3. Experimental results

3.1. Characterization of the samples

In a $< 2\ \mu\text{m}$ fraction of the Majadas sample, only kaolinite is detected by XRD. This mineral is very well ordered and close to the T polytype. The Hinckley index is 1.28 and the Lietard index is 0.88. Electron microscopy shows an excellent hexagonal morphology with a particle size in the $0.1\text{--}1\ \mu\text{m}$ range (Fig. 1a).

The $< 5\ \mu\text{m}$ fraction of the Caobar sample is composed of 98% kaolinite, 1% mica and 1% quartz. This mineral is well-ordered T polytype with Hinckley and Lietard indices of 1.16 and 0.80, respectively. The sample presents an excellent morphology with particle sizes in the $0.5\text{--}2\ \mu\text{m}$ range (Fig. 1b).

The $< 2\ \mu\text{m}$ fraction of the Valdecabras sample comprises 98% kaolinite and 2% quartz. The mineral

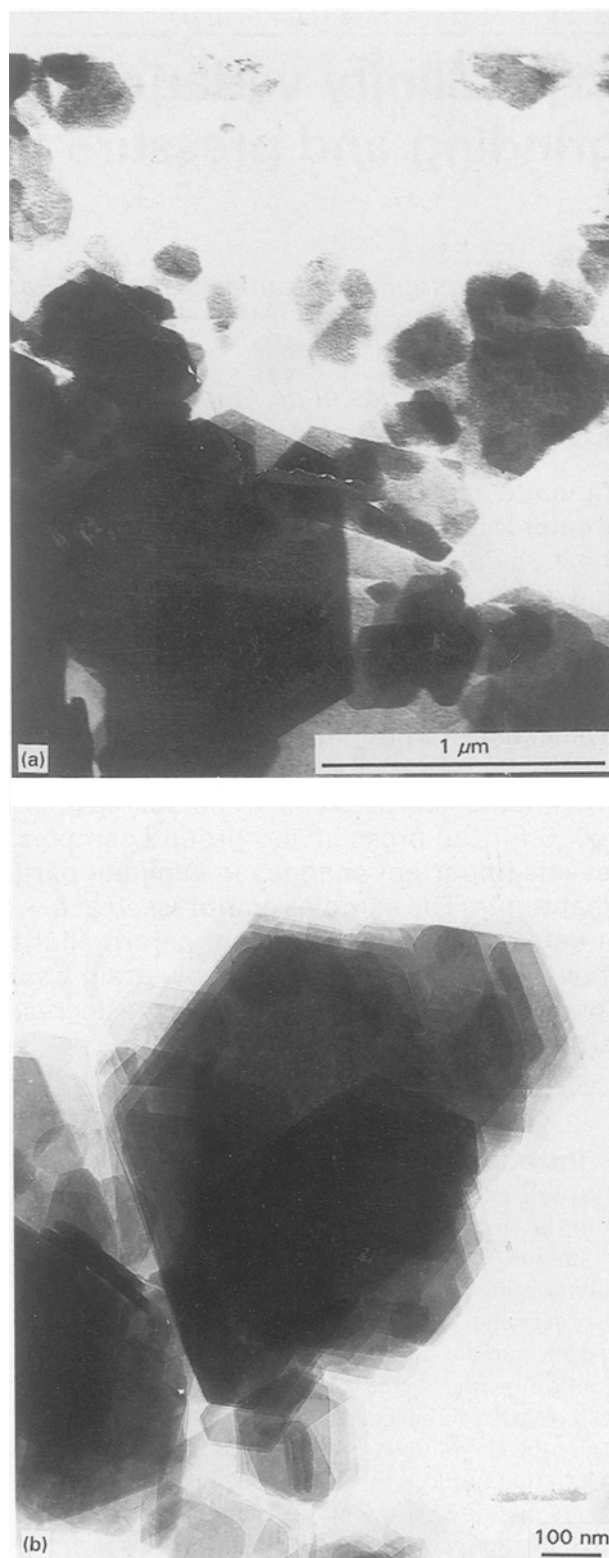


Figure 1 TEM photographs of (a) hexagonal crystals of Majadas kaolinite sample; (b) hexagonal crystals of Caobar kaolinite sample.

presents an ordered T polytype with an Hinckley index of 1.06 and a Lietard index of 1.11. This sample displays an irregular morphology with only 20–30% of hexagonal crystals. The particle size varies from $0.2\text{--}1\ \mu\text{m}$.

The $< 5\ \mu\text{m}$ fraction of the Georgia sample is composed of 98–99% kaolinite and the rest consists of anatase, mica and quartz. The mineral is an ordered polytype with 0.82 and 0.71 Hinckley and Lietard

TABLE I Chemical analysis of kaolinite samples

| | Caobar % | Georgia % | Majadas % | Valdecabras % |
|--------------------------------|----------|-----------|-----------|---------------|
| SiO ₂ | 46.02 | 44.83 | 46.02 | 45.61 |
| Al ₂ O ₃ | 40.03 | 39.31 | 37.52 | 38.39 |
| Fe ₂ O ₃ | 0.25 | 0.36 | 0.80 | 0.92 |
| TiO ₂ | — | 1.20 | — | — |
| CaO | 0.10 | tr | tr | tr |
| MgO | 0.07 | 0.07 | 0.42 | 0.61 |
| K ₂ O | 0.27 | 0.09 | 0.19 | 0.23 |
| Na ₂ O | 0.07 | 0.44 | 0.23 | 0.33 |
| loss at | 13.10 | 13.80 | 14.31 | 13.98 |
| | 99.91 | 100.10 | 99.49 | 100.07 |

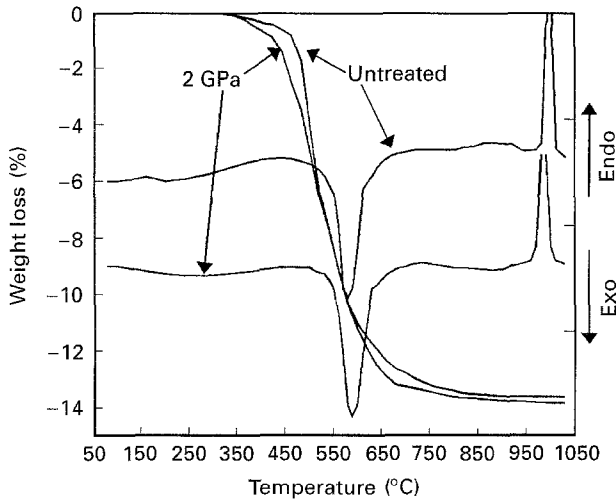


Figure 2 DTA and TGA diagrams of the Caobar kaolinite untreated and after 2.0 GPa pressure treatment.

indices, respectively. The particle size varies in the 0.2–1 μm range and presents an irregular morphology.

Table 1 shows chemical analyses of the four investigated samples. For the four samples, a correlation between the FTIR band at 3695 cm⁻¹ (ν_1 symmetrical vibrations in phase of the OH belonging to the gibbsite-like sheet) and the Hinckley index is shown. Similar behaviour has been observed in reference [20] in well crystallized kaolins, although at lower frequencies.

3.2. Thermal analysis

DTA and TGA data for the Majadas samples (untreated and ground for 1, 2, 4 and 8 h) are shown in Fig. 2. The data for the Caobar samples (untreated and pressed at 0.1, 0.32, 0.85 and 2.0 GPa) are plotted in Fig. 3. Table II shows the temperatures of endothermic and exothermic effects and percentage weight loss for all the studied samples.

The DTA curves of untreated and pressed Caobar samples are very similar and correspond to a highly crystalline kaolinite. Small temperature shifts in the endothermic effects (observed between 581.3–590.4 °C) fall within experimental error. In the same way, small variations in the percentage weight loss are close to those estimated for experimental error. However, TGA experiments are more sensitive to pressure vari-

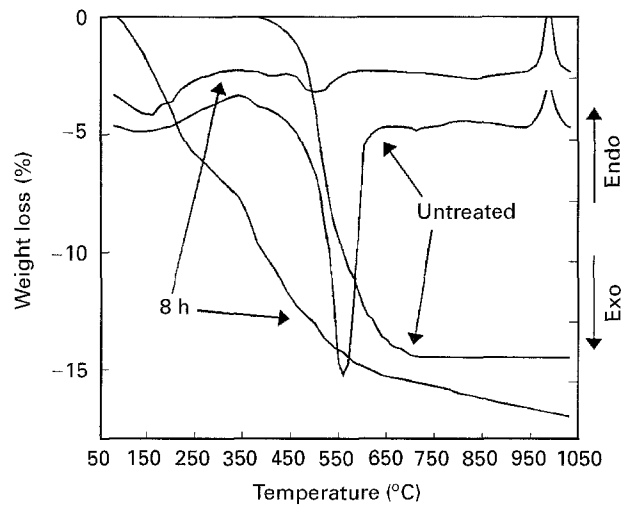


Figure 3 DTA and TGA diagrams of the Majadas kaolinite untreated and grinding treatment after 8 h.

TABLE II DTA and TGA curves. Endothermic and exothermic effects and the percentage weight loss of all studied samples

| Sample | $T_{\text{endo}}(^{\circ}\text{C})$ | $T_{\text{exo}}(^{\circ}\text{C})$ | % weight loss |
|-----------------------------|-------------------------------------|------------------------------------|---------------|
| Caobar untreated | 590.4 | 982.0 | 13.77 |
| Caobar pressed at 0.1 GPa | 584.2 | 974.4 | 14.14 |
| Caobar pressed at 0.32 GPa | 584.8 | 985.8 | 13.68 |
| Caobar pressed at 0.85 GPa | 581.3 | 985.5 | 13.95 |
| Caobar pressed at 2.0 GPa | 582.4 | 984.3 | 13.56 |
| Majadas untreated | 566.2 | 976.4 | 14.06 |
| Majadas ground for 1 h | 526.0 | 978.5 | 14.21 |
| Majadas ground for 2 h | 512.8 | 977.6 | 15.56 |
| Majadas ground for 4 h | 507.4 | 980.8 | 16.50 |
| Majadas ground for 8 h | 500.8 | 982.2 | 16.41 |
| Valdecabras untreated | 542.1 | 986.4 | 13.86 |
| Valdecabras ground for 1 h | 511.4 | 986.2 | 13.23 |
| Valdecabras ground for 3 h | 502.3 | 992.4 | 14.42 |
| Valdecabras ground for 5 h | 493.2 | 988.2 | 14.89 |
| Valdecabras ground for 12 h | 481.6 | 995.2 | 15.66 |

ations than are DTA experiments. From those results it is observed that weight loss begins at lower temperatures in samples treated under high pressure. Thus, an increase of pressure of 2.0 GPa diminishes the dehydroxylation temperature by about 150 °C.

DTA curves of ground Caobar samples are very different from those of the untreated sample. Strong grinding in this sample lowers by 50 °C the temperature of the endothermic effect, it also decreases the

TABLE III Values of HI*, R₂*, RIR*, I₉₃₆/I₉₁₅* and I₇₉₂/I₇₅₅* indices for the different samples

| Sample | HI* | R ₂ * | RIR* | I ₉₃₆ /I ₉₁₅ * | I ₇₉₂ /I ₇₅₅ * |
|-----------------------|------|------------------|------|--------------------------------------|--------------------------------------|
| Caobar untreated | 1.00 | 1.00 | 1.00 | — | 1.00 |
| " 0.1 GPa | 0.69 | 0.97 | 0.89 | — | 1.00 |
| " 0.2 GPa | 0.55 | 0.90 | 0.82 | — | 0.97 |
| " 0.32 GPa | 0.50 | 0.86 | 0.74 | — | — |
| " 0.85 GPa | 0.38 | 0.75 | 0.59 | — | 0.84 |
| " 1.0 GPa | 0.36 | 0.72 | 0.57 | — | 0.83 |
| " 2.0 GPa | 0.29 | 0.69 | 0.54 | — | 0.81 |
| Georgia untreated | 1.00 | 1.00 | 1.00 | — | — |
| " 0.1 GPa | 0.87 | 0.94 | 0.88 | — | — |
| " 0.2 GPa | 0.78 | 0.90 | 0.73 | — | — |
| " 0.32 GPa | 0.70 | 0.86 | 0.62 | — | — |
| " 0.8 GPa | 0.52 | 0.72 | 0.53 | — | — |
| Georgia untreated [9] | 1.00 | 1.00 | — | — | — |
| " 0.05 GPa | 0.91 | 0.92 | — | — | — |
| " 0.1 GPa | 0.74 | 0.92 | — | — | — |
| " 0.2 GPa | 0.55 | 0.83 | — | — | — |
| " 0.6 GPa | 0.46 | 0.80 | — | — | — |
| " 1.0 GPa | 0.41 | 0.76 | — | — | — |
| " 1.5 GPa | 0.40 | 0.72 | — | — | — |
| Majadas untreated | 1.00 | 1.00 | 1.00 | 1.00 | 1.00 |
| " 0.3h | 0.68 | 0.81 | 0.70 | 0.97 | — |
| " 1 h | 0.48 | 0.73 | 0.52 | 0.88 | 0.98 |
| " 2 h | 0.38 | 0.70 | 0.36 | 0.82 | 0.87 |
| " 4 h | 0.23 | 0.65 | 0.26 | 0.64 | 0.82 |
| " 8 h | 0.16 | 0.59 | 0.17 | 0.48 | 0.61 |
| Valdecabras untreated | 1.00 | 1.00 | 1.00 | 1.00 | — |
| " 1 h | 0.53 | 0.73 | 0.50 | 0.91 | — |
| " 3 h | 0.32 | 0.68 | 0.38 | 0.84 | — |
| " 5 h | 0.25 | 0.56 | 0.28 | 0.63 | — |
| " 8 h | 0.19 | 0.44 | — | 0.59 | — |
| " 12 h | — | — | — | — | — |

peak area and raises by 10 °C the temperature of the exothermic effect. The TGA diagrams of ground Caobar samples clearly show a lowering of the starting point for the weight loss and the disappearance of the step at 600 °C. The results obtained on the endothermic effect for ground samples are similar to those published in reference [7] and reference [9].

3.3. X-ray diffraction

Table III presents the calculated Hinckley and Lietard indices and reference intensity ratio values of all the investigated samples. These values have been normalized to the untreated samples (HI*, R₂* and RIR*).

From Figs 4 and 5 it is deduced that the largest changes in the ground samples occur in the 0–2 h interval. In pressed samples (Figs 6 and 7) changes appear when the pressure is varied from 0–0.4 GPa. This behaviour suggests a non linear response of the material with grinding and pressure. Logarithmic regression ($y = a + b \log x$) has been employed to relate the structural variations with grinding time and pressure. Correlation coefficients ($r^{1/2}$) are in the 0.87–1.0 range (Table IV). The b coefficient in the equation is proportional to the rate in the index variation with grinding time or pressure. Examination of the b coefficient for the different indices allows us to evaluate their sensitivity to the grinding and pressure. For the

ground samples (Majadas and Valdecabras kaolinites) and also for the pressed samples (Caobar and Georgia kaolinites) the sequence in the sensitivity of the indices is the following: HI* \geq RIR* > R₂*. This implies that the Hinckley index is the most sensible one to use in order to determine the disorder introduced in the sample by grinding or pressure.

3.4. Infrared spectroscopy

Fig. 4 shows the changes in the intensity for the bands at 936 cm⁻¹ and 915 cm⁻¹ (I₉₃₆/I₉₁₅) and at 792 cm⁻¹ and 755 cm⁻¹ (I₇₉₂/I₇₅₅) with grinding time for the Majadas kaolin. These indices show a logarithmic dependence with the grinding time whose b coefficient is given in Table IV. A similar behaviour with grinding time was observed for the Valdecabras kaolinite (Fig. 5 and Table IV).

The I₉₃₆/I₉₁₅ ratio for the pressed samples (Caobar and Georgia kaolinites) does not significantly change with pressure. Similar observations are reported in reference [21] for other kaolinites. However, the I₇₉₂/I₇₅₅ ratio does show variations with pressure treatment (Fig. 6 and Table IV); small changes in the bands appearing in the 1070–1150 cm⁻¹ region are also detected, these bands are assigned to the Si–O–Si in-plane deformation mode that has been related to structural disorder [19].

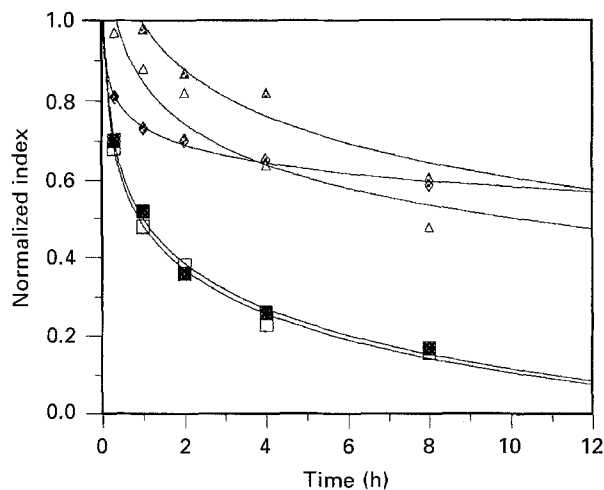


Figure 4 HI* (\square), R_2^* (\blacklozenge), RIR* (\blacksquare), I_{936}/I_{915}^* (\triangle) and I_{792}/I_{755}^* (\blacktriangle) index variations with grinding time for the Majadas kaolinite.

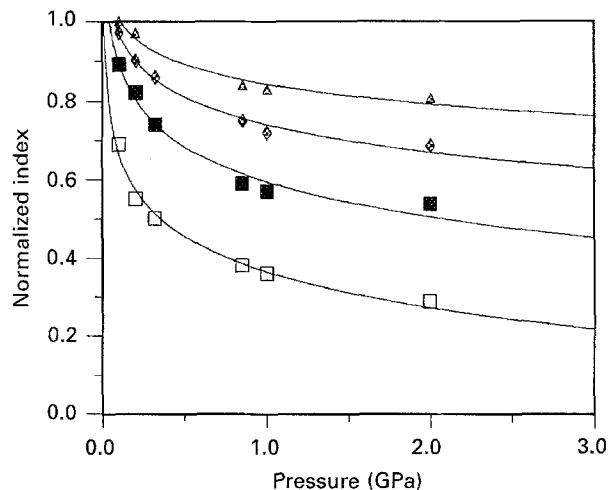


Figure 6 HI* (\square), R_2^* (\blacklozenge), RIR* (\blacksquare), and I_{792}/I_{755}^* (\blacktriangle) index variations with pressure treatments for the Caobar kaolinite.

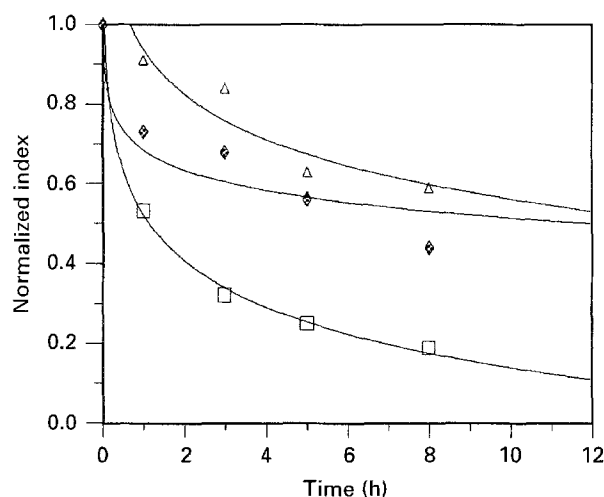


Figure 5 HI* (\square), R_2^* (\blacklozenge), RIR* (\blacksquare) and I_{936}/I_{915}^* (\triangle) index variations with grinding time for the Valdecabras kaolinite.

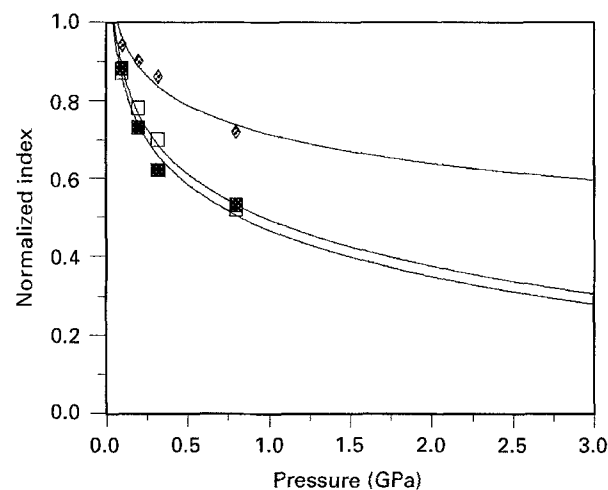


Figure 7 HI* (\square), R_2^* (\blacklozenge) and RIR* (\blacksquare) index variations with pressure treatments for the Georgia kaolinite.

3.5. Electron microscopy

TEM investigations show that the ground samples completely lose the hexagonal morphology of the crystals after two hours treatment. Grinding produces an excess of surface energy that drives together the particles thus producing bunched aggregates of about 1 or 2 μm (Fig. 8a). The formation of bunched aggregates in the first steps of kaolinite grinding has also been reported in reference [7]. As the grinding time increases the particles and the bunched aggregates become smaller and some very small particles ($< 0.05 \mu\text{m}$) can be observed. In some of these crystals

very eroded regions (voids) appear that seem like bubbles. The number of the voids increases with the degree of grinding of the kaolinite (Fig. 8b). These voids cannot be attributed to an agglomeration of point defects because it is too large in size (40–50 nm). The lack of material in these voids suggests a partial dehydroxylation of the octahedral layers.

In the TEM study of the ground samples other defects can be observed, these include grain boundaries, twins, and dislocations. The presence of a large concentration of defects suggests structural disorder and justifies the loss of crystallinity observed in the XRD experiments.

TABLE IV b and r coefficients of the logarithmic regression equation

| Index | Majadas | | Valdecabras | | Caobar | | Georgia | | Georgia [9] | |
|-------------------|---------|-----------|-------------|-----------|--------|-----------|---------|-----------|-------------|-----------|
| | b | $r^{1/2}$ | b | $r^{1/2}$ | b | $r^{1/2}$ | b | $r^{1/2}$ | b | $r^{1/2}$ |
| HI | -0.37 | 0.994 | -0.38 | 0.990 | -0.30 | 0.984 | -0.39 | 0.990 | -0.34 | 0.924 |
| R_2 | -0.15 | 0.991 | -0.17 | 0.905 | -0.23 | 0.987 | -0.25 | 0.945 | -0.14 | 0.949 |
| RIR | -0.38 | 0.992 | -0.30 | 0.976 | -0.30 | 0.974 | -0.39 | 0.958 | - | - |
| I_{792}/I_{755} | -0.39 | 0.932 | - | - | -0.16 | 0.973 | - | - | - | - |
| I_{936}/I_{915} | -0.34 | 0.914 | -0.38 | 0.870 | - | - | - | - | - | - |

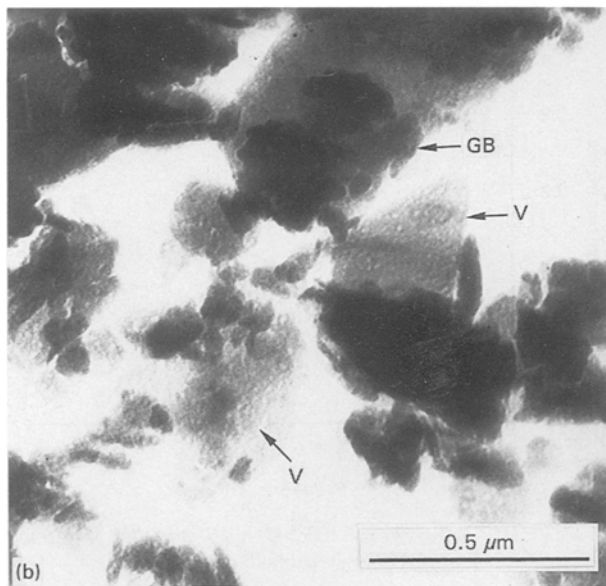
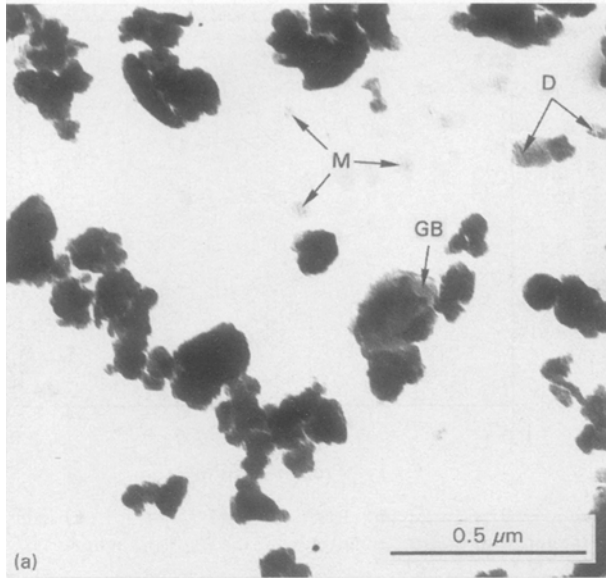


Figure 8 TEM photographs of (a) Majadas sample after 4 h grinding; (b) Valdecabras sample after 8 h grinding; grain boundaries (GB), dislocations (D), micro crystals about 30 nm diameter (M) and rounded void (V).

A TEM study of the sample pressed at 0.32 GPa shows the presence of large bent crystals which sometime are even rolled in their borders. Occasionally the large crystals lose their hexagonal habit due to longitudinal fractures. The sample pressed at 0.85 GPa shows many bent crystals forming tube like halloysite and sometimes they are broken as is shown in Fig. 9a. Nevertheless, the very small crystals ($< 0.1 \mu\text{m}$) do not show any changes as is also shown in Fig. 9a. For higher pressures such as 1.0 GPa many of the large crystals become broken, bent, deformed and even the small crystals show some alterations. For instance, in the Caobar sample pressed at 2.0 GPa many defects and bubbles can be observed which is similar behaviour to that observed in the ground samples suggesting a great deal of structural disorder (Fig. 9b). From the electron diffraction studies differences between the ground and pressed samples can be detected. In general ground samples produce patterns

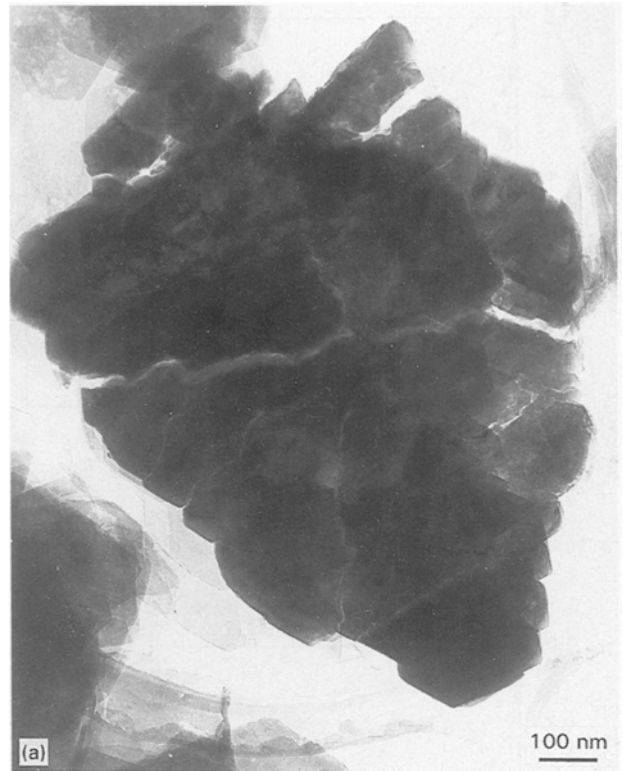


Figure 9 TEM photographs of (a) bent and broken crystals in the Caobar kaolinite sample pressed at 0.85 GPa; (b) kaolinite sample pressed at 2.0 GPa.

containing a few irregular spots indicating the loss of periodicity in the structure.

4. Discussion and conclusions

From the XRD, thermal analysis (DTA and TGA), FTIR, and TEM experimental results it can be concluded that grinding and pressure treatments of

kaolinite produce important changes in the morphology, structure and crystallinity of the samples. Grinding is more destructive than pressure treatments in the range studied here. Thus, thermograms, and HI, R₂, RIR, I₉₃₆/I₉₁₅ and I₇₉₂/I₇₅₅ indices show bigger changes in ground samples for which the morphology of the crystals is impaired after short grinding times.

The DTA curves of pressed kaolinites remain almost unchanged with pressure treatment. In the TGA diagrams of these samples only a lowering in the starting temperature of the weight loss is observed. On the contrary, the DTA curves of ground kaolinites show (i) a decrease in the temperature and intensity of the endothermic process, and (ii) an increase of the temperature of the exothermic process, with increasing grinding time. In addition, for samples ground for longer than 4 h a new endothermic process at about 200 °C is also observed. The TGA diagrams of ground samples also show the same effects i.e., a lower temperature and a smaller slope in the weight loss process and a larger total weight loss (Fig. 2).

The dehydroxylation temperature is lower in both ground and pressed kaolinites. Both treatments produce changes in the crystalline structure that facilitate the elimination of OH groups. Few alterations must occur in pressed kaolinites because their TGA diagrams show little change as compared to the untreated samples. In ground kaolinites the structural modifications are very important affecting both endothermic and exothermic processes (Table II). The changes in the exothermic effect could be explained by taking into account that similar large structural disorder in the samples created difficulties in attempts to recrystallize mullite.

The electron microscopy studies show that grinding impairs the morphology of the crystals giving very small sized particles. A pressure treatment produces only small changes in the morphology of the crystals.

In the same manner to that observed for ground kaolinites the XRD patterns of the pressed samples indicate a strong decrease in the HI, R₂ and RIR indices. However, these changes do not significantly alter the thermal properties and crystalline morphology. IR spectroscopy show small modifications in the position or the intensity of the bands. This apparent contradiction can be explained if the high pressures only affects the (*a**, *b**) planes. Meanwhile, grinding produces: (i) impairment of the morphology and reduction of particle size, (ii) periodicity disorder and (iii) short range disorder. This last effect is related to

variations in the coordination shell of the atoms and justifies the formation of amorphous phases. NMR spectroscopy can be used to detect these changes and in reference [6] it is demonstrated that aluminium atoms can change from a VI to a IV coordination during the grinding process. In the same way reference [10] has also demonstrated that pressure treatment does not affect aluminium coordination in kaolinite.

References

1. W. D. LAWS and J. B. PAGE, *Soil Sci.* **62** (1946) 319.
2. S. J. GREGG, K. F. HILL and T. V. PARKER, *J. Appl. Chem.* **4** (1954) 666.
3. H. KODAMA and M. JAAKKIMAINEN, in Proceedings International Clay Conference Bologna, Pavia 1981, edited by H. van Olphen and F. Veniale (Elsevier, Amsterdam, 1982) p. 399.
4. S. DE LUCA and M. SLAUGHTER, *Amer. Miner.* **70** (1985) 149.
5. R. T. TETTENHORST and C. E. CORBATÓ, *Clay Minerals* **21** (1986) 971.
6. H. KODAMA, L. S. KOTLYAR and J. A. RIPMEESTER, *Clays Clay Min.* **37** (1989) 364.
7. F. GONZALEZ GARCÍA, M. T. RUIZ ABRIO and M. GONZALEZ RODRIGUEZ, *Clay Minerals* **26** (1991) 549.
8. E. KRISTÓF, Z. JUHÁSZ and I. VASSÁNYI, *Clays Clay Min.* **41** (1993).
9. K. J. RANGE, A. RANGE and A. WEISS, in Proceedings International Clay Conference, Tokyo, 1969, edited by L. Heller (Israel Univ. Press, Jerusalem, 1969) p. 3.
10. A. LA IGLESIA, *Clay Minerals* **28** (1993) 311.
11. E. GALÁN, Ph.D. thesis, Univ. Complutense, Spain (1972).
12. S. LEGUEY and M. DOVAL, in 6th Meet. Europ. Clay Groups, "Guidebook for Excursions", Sevilla, September 1987, edited by J. L. Perez-Rodríguez and E. Galan (Ortega, 1987) 138.
13. S. H. PATTERSON and H. H. MURRAY, "Industrial minerals and rocks" (AIME, New York, 1975).
14. D. N. HINCKLEY, *Clays Clay Min.* **13** (1963) 229.
15. O. LIETARD, Ph.D. thesis. (Nancy, 1977).
16. B. L. DAVIS and D. K. SMITH, *Power Diffraction* **3** (1988) 205.
17. B. L. DAVIS, D. K. SMITH and M. A. HOLOMANY, *ibid.* **4** (1989) 201.
18. C. A. HUBBARD, E. H. EVANS and D. K. SMITH, *J. Appl. Cryst.* **9** (1976) 169.
19. V. C. FARMER and J. D. RUSSELL, *Spectrochim. Acta* **20** (1964) 1149.
20. G. W. BRINDLEY, C. C. KAO, J. L. HARRISON, M. LIPICAS and R. RAYTHATHA, *Clays Clay Min.* **34** (1986) 239.
21. V. A. BELL, V. R. CITRO and G. D. HODGE, *ibid.* **39** (1991) 290.

Received 2 August 1994
and accepted 13 February 1996